Inorganic Chemistry

Article

pubs.acs.org/IC

Tetranuclear Lanthanide(III) Complexes with a Zigzag Topology from the Use of Pyridine-2,6-dimethanol: Synthetic, Structural, Spectroscopic, Magnetic and Photoluminescence Studies

Dimitris I. Alexandropoulos,[†] Luís Cunha-Silva,[‡] Linh Pham,[§] Vlasoula Bekiari,[∥] George Christou,[§] and Theocharis C. Stamatatos*,[†]

[†]Department of Chemistry, Brock University, L2S 3A1 St. Catharines, Ontario, Canada

[‡]REQUIMTE & Department of Chemistry and Biochemistry, Faculty of Sciences, University of Porto, 4169-007 Porto, Portugal

[§]Department of Chemistry, University of Florida, Gainesville, Florida 32611-7200, United States

[∥]Department of Aquaculture and Fisheries Management, Technological Educational Institute of Western Greece, 30 200 Messolonghi, Greece

Supporting Information

ABSTRACT: Reaction between $Ln(NO_3)_3{\cdot}xH_2O$ (x = 5 or 6) and the potentially tridentate (N,O,O) chelating/bridging ligand pyridine-2,6-dimethanol ($pdmH_2$), in the presence of base NEt_3, affords a family of isostructural tetranuclear $[Ln^{III}_4(NO_3)_2(pdmH)_6(pdmH_2)_2](NO_3)_4$ (Ln^{III} = Eu^{III}, Gd^{III}, Tb^{III}, Dy^{III}, Ho^{III}, Er^{III}, Yb^{III}) complexes with a rare zigzag topology. All complexes contain a $[Ln_4(\mu\text{-}OR)_6]^{6+}$ core with bridging ligation provided by the alkoxido arms of six $\eta^1{:}\eta^1{:}\eta^2{:}\mu$ $pdmH^-$ groups. The Ln^{III} ions are eight coordinate with distorted geometries. Direct current magnetic susceptibility studies revealed predominant weak antiferromagnetic exchange interactions between the metal centers, which were quantified in the case of isotropic Gd^{III}_4 to give $J = -0.09(1)$ cm^{-1} and $g = 2.00(1)$. The observation of out-of-phase (χ''_M) ac susceptibility signals suggested that the Dy^{III}_4 analogue might be a molecular nanomagnet. Solid-state photoluminescence studies showed that the Eu^{III}_4 and Tb^{III}_4 compounds exhibit intense, sharp, and narrow emission bands in the red and green visible regions, respectively, which arise from the characteristic $^5D_0 \rightarrow {}^7F_J$ and $^5D_4 \rightarrow {}^7F_J$ transitions. The combined results demonstrate the ability of $pdmH_2$ ligand to yield homometallic 4f clusters with interesting magnetic and optical properties.

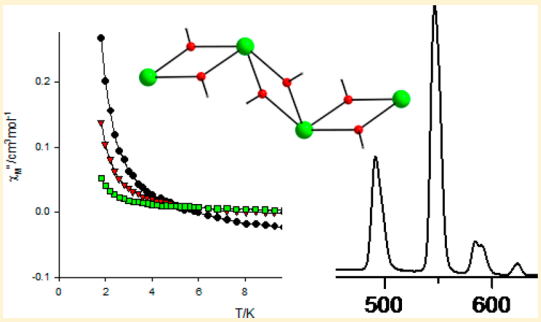

INTRODUCTION

Lanthanide (Ln) coordination chemistry is undoubtedly on the forefront of modern fundamental and applied research.[1] This is due to the ability of 4f-metal coordination complexes to find applications in various fields of science, such as medicinal chemistry, biology, optics, catalysis, and magnetism.[2] Polynuclear homometallic lanthanide complexes (or 4f-metal clusters) is a class of coordination compounds that comprises high-nuclearity (number of metal ions ≥ 3)[3] molecular species with aesthetically pleasing structures, exotic topologies, and beautiful mosaics. Occasionally, such compounds partly or fully resemble the structural motifs found in Platonic,[4] Archimedean,[5] and Johnson solids.[6] Their nature and often nanoscale dimensions bring to the field of nanoscale materials all the advantages of a molecular, "bottom-up" approach,[7] such as monodispersity, "low-energy" synthetic conditions, solubility, "tailoring" ability, and crystallinity.

The different electronic and physical properties of the 4f-metal ions can lead to a wide variety of interesting potential applications. For example, Ln^{III} clusters have shown a remarkable ability to act either as single-molecule magnets (SMMs)[8] when the f-block ions are highly anisotropic and carry a significant spin (i.e., Dy^{III}, Tb^{III}, Ho^{III}, Er^{III}) or as molecular magnetic coolers[9] when the molecules are isotropic and high spin, prerequisites which are fulfilled by utilization of the Gd^{III} ion. Restricting further discussion to the former area, SMMs derive their properties from the combination of a large magnetic moment in the ground state with a large magnetoanisotropy originating from the substantial, unquenched orbital angular momenta.[8,10] As a result, 4f-SMMs often possess an appreciable barrier to magnetization relaxation at low temperatures, and they display out-of-phase ac magnetic susceptibility signals and hysteresis loops in magnetization vs applied dc fields.[11] Due to a combination of interesting classical and quantum properties, such as quantum tunneling of magnetization (QTM)[12] and quantum phase interference,[13] SMMs have been proposed for a variety of potential advanced applications, including molecular spintronics and quantum computation.[14]

Received: January 15, 2014
Published: February 24, 2014

   dx.doi.org/10.1021/ic5001045 | Inorg. Chem. 2014, 53, 3220−3229

Polynuclear 4f-metal complexes have also shown intense and long-lived emissions, which make these compounds particularly interesting for a variety of optical and medical uses such as display devices, luminescent sensors, and probes for clinical use.[15] This applies significantly to Eu^{III}- and Tb^{III}-based clusters with red and green luminescence due to $^5D_0 \rightarrow {}^7F_J$ and $^5D_4 \rightarrow {}^7F_J$ transitions, respectively,[2,16] and occasionally to Dy^{III} complexes with characteristic $^4F_{9/2} \rightarrow {}^6H_J$ transitions[2,17] appearing at the blue or yellow regions of the visible spectrum. Luminescence from Ln^{III} ions results from electronic transitions between the 4f orbitals; however, such transitions are forbidden on symmetry grounds and lead to poor absorption cross sections and excited states with long lifetimes.[18] Consequently, the desired population of the emitting levels of the Ln^{III} ion is best achieved by employing light-harvesting ligands which can absorb strongly UV light and therefore sensitize the metal ion by intramolecular energy transfer from the ligand-based triplet state.[19] Therefore, access to "hybrid" molecular materials with both intriguing magnetic (i.e., SMM behavior) and optical properties (i.e., emission in the visible region) can be potentially accomplished when the 4f-metal ion is either Tb^{III} or Dy^{III}.[11b,c,20]

The chances of synthesizing new Ln^{III} clusters with both interesting magnetic and optical properties should be enhanced by development of new reaction schemes with suitable organic bridging/chelating ligands. For construction of such "hybrid" molecular materials, the choice of the organic ligand is of fundamental importance. This should present (i) a binding affinity to the oxophilic Ln^{III} ions by containing O-donor atom(s), (ii) a multimetal center bridging capability with simultaneous prevention of polymer formation, and (iii) an ability to both propagate strong magnetic exchange interactions between the metal atoms it bridges and contain aromatic group(s) to enhance the luminescence intensities and lifetimes.[21]

Following our longstanding interest in the coordination ability/affinity of pyridyl alcohols[22] and pyridyl oximes/dioximes[23] for metal cluster synthesis, we decided to employ pyridine-2,6-dimethanol ($pdmH_2$, Scheme 1), a well-known ligand for synthesis of 3d-metal clusters and SMMs[24] but with scant previous use in homometallic 4f-metal cluster chemistry.[25] Herein we report the syntheses, structures, magnetic, and photoluminescence properties of a family of isostructural tetranuclear $[Ln^{III}_4(NO_3)_2(pdmH)_6(pdmH_2)_2](NO_3)_4$ (Ln^{III} = Eu^{III}, Gd^{III}, Tb^{III}, Dy^{III}, Ho^{III}, Er^{III}, Yb^{III}) complexes with a rare zigzag topology. The combined results demonstrate the ability of $pdmH_2$ to yield 4f-metal clusters with SMM and photoluminescence behaviors, without requiring the copresence of ancillary bridging ligands, such as carboxylates, β-diketonates, and/or pseudohalides.

Scheme 1. Structural Formula and Abbreviation of the Ligand Pyridine-2,6-dimethanol ($pdmH_2$) Used in This Study

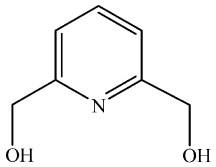

$pdmH_2$

EXPERIMENTAL SECTION

Synthesis. All manipulations were performed under aerobic conditions using chemicals and solvents as received.

*$[Eu_4(NO_3)_2(pdmH)_6(pdmH_2)_2](NO_3)_4$ (**1**).* To a stirred, colorless solution of $pdmH_2$ (0.14 g, 1.0 mmol) and NEt_3 (0.14 mL, 1.0 mmol) in MeOH (20 mL) was added solid $Eu(NO_3)_3{\cdot}5H_2O$ (0.21 g, 0.5 mmol). The resulting pale yellow solution was kept under stirring at room temperature for about 20 min and filtered, and the filtrate was layered with Et_2O (40 mL). Slow mixing gave after 2 days colorless prismatic crystals of **1**, which were not of sufficient quality to allow acquisition of a complete X-ray diffraction data set. Crystals were collected by filtration, washed with cold MeOH (2 × 2 mL) and Et_2O (2 × 3 mL), and dried in air; the yield was 60%. The identity of the product was confirmed by (i) a unit cell determination and comparison with the unit cell of compound **3**·2MeOH, (ii) IR spectroscopic comparison with all isostructural Ln_4 complexes, and (iii) elemental analysis (see below). The air-dried solid was analyzed as solvent-free **1**. Anal. Calcd: C, 32.23; H, 3.19; N, 9.40. Found: C, 32.04; H, 3.05; N, 9.56.

*$[Gd_4(NO_3)_2(pdmH)_6(pdmH_2)_2](NO_3)_4$ (**2**).* This complex was prepared in the same manner as complex **1** but using $Gd(NO_3)_3{\cdot}6H_2O$ (0.23 g, 0.5 mmol) as the Ln salt. Due to the small size of the colorless crystals formed after 3 days and consequently the weak overall diffraction, we were not able to collect a complete X-ray data set. Crystals were collected by filtration, washed with cold MeOH (2 × 2 mL) and Et_2O (2 × 3 mL), and dried in air; the yield was 50%. The identity of the product was confirmed by the same means we followed for structural determination of complex **1**. The air-dried solid was analyzed as **2**·2MeOH. Anal. Calcd: C, 32.07; H, 3.43; N, 9.03. Found: C, 32.16; H, 3.53; N, 8.75.

*$[Tb_4(NO_3)_2(pdmH)_6(pdmH_2)_2](NO_3)_4$ (**3**).* This complex was prepared in the same manner as complex **1** but using $Tb(NO_3)_3{\cdot}6H_2O$ (0.23 g, 0.5 mmol) as the Ln salt. After 3 days, X-ray-quality colorless crystals of **3**·2MeOH appeared and were collected by filtration, washed with cold MeOH (2 × 2 mL) and Et_2O (2 × 3 mL), and dried in air; the yield was 60%. The air-dried solid was analyzed as **3**·2MeOH. Anal. Calcd: C, 31.97; H, 3.42; N, 9.00. Found: C, 32.26; H, 3.52; N, 8.79. Selected IR data (cm^{-1}): 3450 (wb), 3050 (m), 2923 (w), 1579 (s), 1519 (vs), 1479 (m), 1423 (m), 1388 (s), 1340 (w), 1321 (s), 1276 (m), 1224 (w), 1200 (w), 1074 (w), 1014 (w), 943 (w), 887 (w), 846 (w), 730 (m), 674 (m), 622 (m), 574 (w), 501 (w), 451 (w). UV−vis (λ/nm in MeCN): 224, 270.

*$[Dy_4(NO_3)_2(pdmH)_6(pdmH_2)_2](NO_3)_4$ (**4**).* This complex was prepared in the same manner as complex **1** but using $Dy(NO_3)_3{\cdot}6H_2O$ (0.23 g, 0.5 mmol) as the Ln salt. Colorless prismatic crystals of **4** appeared after 4 days and were collected by filtration, washed with cold MeOH (2 × 2 mL) and Et_2O (2 × 3 mL), and dried in air; the yield was 70%. Due to the small size and phase homogeneity issues (i.e., twinning) of the crystals, we were not able to collect an accurate, complete X-ray data set. However, the identity of the product was confirmed by (i) unit cell determination and comparison with the unit cell of compound **5**·2MeOH, (ii) IR spectroscopic comparison with all isostructural Ln_4 complexes, and (iii) elemental analysis (see below). The air-dried solid was analyzed as solvent-free **4**. Anal. Calcd: C, 31.59; H, 3.12; N, 9.21. Found: C, 31.73; H, 3.15; N, 9.01.

*$[Ho_4(NO_3)_2(pdmH)_6(pdmH_2)_2](NO_3)_4$ (**5**).* This complex was prepared in the same manner as complex **1** but using $Ho(NO_3)_3{\cdot}5H_2O$ (0.22 g, 0.5 mmol) as the Ln salt. After 2 days, X-ray-quality colorless crystals of **5**·2MeOH appeared and were collected by filtration, washed with cold MeOH (2 × 2 mL) and Et_2O (2 × 3 mL), and dried in air; the yield was 65%. The air-dried solid was analyzed as solvent-free **5**. Anal. Calcd: C, 31.45; H, 3.11; N, 9.17. Found: C, 31.08; H, 2.91; N, 9.43. Selected IR data (cm^{-1}): 3444 (wb), 3050 (m), 2925 (w), 1579 (s), 1519 (vs), 1481 (m), 1423 (m), 1384 (s), 1317 (s), 1276 (m), 1223 (w), 1203 (w), 1072 (w), 1014 (w), 940 (w), 887 (w), 850 (w), 730 (m), 669 (m), 624 (m), 573 (w), 500 (w), 449 (w). UV−vis (λ/nm in MeCN): 223, 264.

*$[Er_4(NO_3)_2(pdmH)_6(pdmH_2)_2](NO_3)_4$ (**6**).* This complex was prepared in the same manner as complex **1** but using $Er(NO_3)_3{\cdot}5H_2O$

dx.doi.org/10.1021/ic5001045 | Inorg. Chem. 2014, 53, 3220−3229

Table 1. Crystallographic Data for Complexes 1−7

	1·2MeOH	**2**·2MeOH	**3**·2MeOH	**4**·2MeOH	**5**·2MeOH	**6**·2MeOH	**7**·2MeOH
formula[a]	$C_{58}H_{74}Eu_4N_{14}O_{36}$	$C_{58}H_{74}Gd_4N_{14}O_{36}$	$C_{58}H_{74}Tb_4N_{14}O_{36}$	$C_{58}H_{74}Dy_4N_{14}O_{36}$	$C_{58}H_{74}Ho_4N_{14}O_{36}$	$C_{58}H_{74}Er_4N_{14}O_{36}$	$C_{58}H_{74}Yb_4N_{14}O_{36}$
fw[a]/g mol^{-1}	2151.15	2172.28	2178.99	2193.28	2203.03	2212.35	2235.47
cryst type	colorless plate	colorless plate	colorless prism	colorless plate	colorless plate	colorless plate	colorless plate
cryst size/mm	0.07 × 0.04 × 0.01	0.08 × 0.05 × 0.01	0.17 × 0.08 × 0.08	0.06 × 0.04 × 0.02	0.08 × 0.05 × 0.02	0.04 × 0.02 × 0.01	0.07 × 0.04 × 0.02
cryst syst	monoclinic	monoclinic	monoclinic	monoclinic	monoclinic	monoclinic	monoclinic
space group			$P2_1/n$		$P2_1/n$	$P2_1$	$P2_1/n$
a/Å	15.484(2)	15.461(2)	15.2655(18)	15.375(2)	15.2459(19)	15.5716(18)	15.287(2)
b/Å	14.941(2)	14.892(2)	14.9732(16)	14.858 (2)	14.8786(18)	14.0309(15)	14.773(2)
c/Å	15.953(2)	15.998(2)	16.0103(19)	15.943(2)	15.983(2)	16.5856(19)	15.954(2)
α/deg	90	90	90	90	90	90	90
β/deg	92.561(6)	92.679(7)	92.407(6)	93.095(7)	92.423(6)	95.035(6)	93.095(7)
γ/deg	90	90	90	90	90	90	90
vol./Å^3	3694.7(9)	3683.5(9)	3656.3(7)	3642.7(9)	3622.3(8)	3609.7(7)	3597.6(9)
Z			2		2	2	2
ρ_{calcd}/g cm^{-3}			1.979		2.020	2.035	2.064
μ/mm^{-1}			3.925		4.426	4.707	5.257
θ range/deg			3.73−28.28		3.74−26.37	3.70−25.68	3.76−26.37
index ranges			$-20 \le h \le 20$		$-19 \le h \le 19$	$-18 \le h \le 18$	$-19 \le h \le 19$
			$-19 \le k \le 19$		$-18 \le k \le 18$	$-16 \le k \le 17$	$-18 \le k \le 18$
			$-21 \le l \le 21$		$-19 \le l \le 19$	$-20 \le l \le 20$	$-19 \le l \le 19$
no. of collected reflns			150 416		166 714	57 169	141 226
no. of independent reflns			9057 (R_{int} = 0.0441)		7388 (R_{int} = 0.0527)	13561 (R_{int} = 0.0502)	7227 (R_{int} = 0.0745)
final $R^{b,e}$ indices [$I > 2\sigma(I)$]			$R1$ = 0.0442		$R1$ = 0.0490	$R1$ = 0.0588	$R1$ = 0.1030
			w$R2$ = 0.0779		w$R2$ = 0.0894	w$R2$ = 0.1266	w$R2$ = 0.1186
final R indices (all data)			$R1$ = 0.0475		$R1$ = 0.0523	$R1$ = 0.0761	$R1$ = 0.1219
			w$R2$ = 0.0797		w$R2$ = 0.0904	w$R2$ = 0.1366	w$R2$ = 0.1322
$(\Delta\rho)_{max,min}$/e Å^{-3}			1.309, −1.195		1.823, −1.713	3.274, −1.108	1.974, −2.435

[a]Including solvate molecules. [b]$R1 = \Sigma(||F_o| - |F_c||)/\Sigma|F_o|$. [e]$wR2 = [\Sigma[w(F_o^2 - F_c^2)^2]/\Sigma[w(F_o^2)^2]]^{1/2}$, $w = 1/[\sigma^2(F_o^2) + (ap)^2 + bp]$, where $p = [\max(F_o^2, 0) + 2F_c^2]/3$.

(0.22 g, 0.5 mmol) as the Ln salt. After 4 days, X-ray-quality colorless crystals of **6**·2MeOH appeared and were collected by filtration, washed with cold MeOH (2 × 2 mL) and Et_2O (2 × 3 mL), and dried in air; the yield was 55%. The air-dried solid was analyzed as solvent-free **6**. Anal. Calcd: C, 31.31; H, 3.10; N, 9.13. Found: C, 31.14; H, 2.95; N, 9.26.

*$[Yb_4(NO_3)_2(pdmH)_6(pdmH_2)_2](NO_3)_4$ (**7**).* This complex was prepared in the same manner as complex **1** but using $Yb(NO_3)_3{\cdot}5H_2O$ (0.23 g, 0.5 mmol) as the Ln salt. After 3 days, X-ray-quality colorless crystals of **7**·2MeOH appeared and were collected by filtration, washed with cold MeOH (2 × 2 mL) and Et_2O (2 × 3 mL), and dried in air; the yield was 75%. The air-dried solid was analyzed as solvent-free **7**. Anal. Calcd: C, 30.98; H, 3.06; N, 9.03. Found: C, 31.21; H, 3.19; N, 8.95.

X-ray Crystallography. Colorless crystals of all reported compounds **1**−**7** were manually harvested and mounted on cryoloops using adequate oil.[26] Diffraction data were collected at 150.0(2) K on a Bruker X8 Kappa APEX II Charge-Coupled Device (CCD) area-detector diffractometer controlled by the APEX2 software package[27] (Mo Kα graphite-monochromated radiation, λ = 0.71073 Å) and equipped with an Oxford Cryosystems Series 700 cryostream monitored remotely with the software interface Cryopad.[28] Images were processed with the software SAINT+,[29] and absorption was corrected using the multiscan semiempirical method implemented in SADABS.[30] Structures were solved by direct or Patterson methods employed in SHELXS-97,[31,32] allowing the immediate location of the heaviest lanthanide elements. The remaining, non-H atoms were located from difference Fourier maps, calculated by full-matrix least-squares refinement cycles on F^2 using SHELXL-97,[32,33] and refined with anisotropic displacement parameters.

In all structures, the H atoms bound to the C atoms of the $pdmH^-$/$pdmH_2$ ligands and MeOH solvate molecules were placed at their geometrical positions using *HFIX* instructions in SHELXL (43 for the aromatic, 23 for the CH_2, and 137 for the terminal CH_3 groups) and included in subsequent refinement cycles in riding-motion approximation with isotropic thermal displacements parameters (U_{iso}) fixed at 1.2 or 1.5 × U_{eq} of the C atom to which they are attached. The H atoms of the hydroxyl groups of $pdmH^-$/$pdmH_2$ ligands were found in difference Fourier maps and placed in the structural model with the O−H distances restrained to 0.85(1) Å or included in their idealized positions. Programs used for molecular graphics were MERCURY[34] and DIAMOND.[35] Unit cell parameters and structure solution and refinement data for all complexes are listed in Table 1. Further crystallographic details can be found in the corresponding CIF files provided in the Supporting Information. Crystallographic data (excluding structure factors) for the structures reported in this work have been deposited to the Cambridge Crystallographic Data Centre (CCDC) as supplementary publication numbers: CCDC-975152 (**3**·2MeOH), 975149 (**5**·2MeOH), 975150 (**6**·2MeOH), and 975151 (**7**·2MeOH).

Physical Measurements. Infrared (IR) spectra were recorded in the solid state (KBr pellet) on a Perkin-Elmer 16 PC FT spectrometer in the 4000−450 cm^{-1} range. Elemental analyses (C, H, and N) were performed on a Perkin-Elmer 2400 Series II Analyzer. UV−visible (UV−vis) spectra were recorded in MeCN solution at concentrations $\approx 10^{-5}$ M on a Beckman Coulter DU Series 700 dual-beam spectrophotometer. Excitation and emission spectra were recorded in the solid state using a Cary Eclipse spectrofluorometer. Direct current (dc) and alternating current (ac) magnetic susceptibility studies were performed at the University of Florida Chemistry

dx.doi.org/10.1021/ic5001045 | Inorg. Chem. 2014, 53, 3220−3229

Department on a Quantum Design MPMS-XL SQUID susceptometer equipped with a 7 T magnet and operating in the 1.8–400 K range. Samples were embedded in solid eicosane to prevent torquing. Alternating current magnetic susceptibility measurements were performed in an oscillating ac field of 3.5 G and a zero dc field. Oscillation frequencies were in the 50–1000 Hz range. Pascal's constants were used to estimate the diamagnetic correction, which was subtracted from the experimental susceptibility to give the molar paramagnetic susceptibility (χ_M).[36]

RESULTS AND DISCUSSION

Synthesis and IR Spectra. Many synthetic procedures to polynuclear 4f-metal complexes rely on reactions of simple LnX_3 starting materials (X^- = various) with a potentially chelating/bridging organic ligand.[11,20,37] The nature of both the X^- group and the organic ligand is of significant synthetic importance. When X^- belongs to the carboxylate or β-diketonate groups, additional bridging ligation from these groups might be provided, resulting in formation of higher nuclearity metal species. Additionally, their strong basic nature fosters deprotonation of the organic chelating/bridging ligand without requiring the use of an external base. On the other hand, when the choice of X^- is one of the halides, NO_3^-, ClO_4^-, or $CF_3SO_3^-$, all with limited bridging affinity, employment of an external organic base which would carry the role of proton acceptor seems necessary to facilitate deprotonation of the organic chelating/bridging ligand and therefore increase the chances of metal cluster formation. The latter route was followed in the present study using as organic chelating/bridging ligand the relatively unexplored in lanthanide metal cluster chemistry pyridine-2,6-dimethanol ($pdmH_2$).[25] The pyridyl diol ligand $pdmH_2$ contains two –OH groups which upon deprotonation could bridge up to five metal centers.[24] Previous use of $pdmH_2$ in 4f-metal cluster chemistry has been limited to the two isostructural carboxylate complexes $[Yb_4(O_2CPh)_2(pdm)_4(pdmH)_2(HO_2CPh)_2(H_2O)_2]$[25b] and $[Dy_4(O_2CPh)_2(pdm)_4(pdmH)_2(HO_2CPh)_4]$,[25a] both with a zigzag topology.

A variety of reactions differing in the metal:$pdmH_2$ ratio, the inorganic ions present, the organic base, and/or the reaction solvent(s) were explored in identifying the following successful system. Reactions of $Ln(NO_3)_3{\cdot}xH_2O$ (x = 5 or 6) with $pdmH_2$ in a 1:2 molar ratio in MeOH in the presence of 2 equiv of NEt_3 gave colorless solutions that, upon filtration and layering with Et_2O, afforded colorless crystals of a family of isostructural tetranuclear $[Ln_4(NO_3)_2(pdmH)_6(pdmH_2)_2](NO_3)_4{\cdot}2MeOH$ [Ln = Eu (**1**); Gd (**2**); Tb (**3**); Dy (**4**); Ho (**5**); Er (**6**); Yb (**7**)] complexes in very good yields (50–75%). The general formation of **1**–**7** is summarized in eq 1.

$$4Ln(NO_3)_3{\cdot}xH_2O + 8pdmH_2 + 6NEt_3 \xrightarrow{MeOH} [Ln_4(NO_3)_2(pdmH)_6(pdmH_2)_2] + 6(NHEt_3)(NO_3) + 4H_2O$$

Ln = Eu(**1**); Gd(**2**); Tb(**3**); Dy(**4**); Ho(**5**); Er(**6**); Yb(**7**); x = 5 or 6 (1)

In an attempt to obtain higher nuclearity Ln^{III} products, several reactions were performed with higher Ln^{III}:$pdmH_2$ ratios, up to 4:1. However, the tetranuclear complexes **1**–**7** were still the only isolable products, in comparable (1:1 or 2:1 ratios) or lower (3:1 or 4:1 ratios) yields. Complexes **1**–**7** were also obtained when the reactions were performed in EtOH (confirmation from IR spectroscopic studies) or a mixture of MeCN/MeOH (2:1, v/v) but in much lower yields (~10–20%), whereas no significant reactions were observed when the solvent was CH_2Cl_2 or $CHCl_3$. An increase in the NEt_3:$pdmH_2$ ratio up to 3:1 gave comparable (or slightly decreased) yields of complexes **1**–**7** rather than higher nuclearity products resulting from complete deprotonation of $pdmH^-/pdmH_2$ groups. Further increases in the amount of NEt_3 gave oily products suggestive of mixtures that we have not been able to characterize or insoluble amorphous precipitates that were probably Ln oxides or oxo/hydroxide species. Replacement of NEt_3 by other organic bases, i.e., Me_4NOH, also led to isolation of **1**–**7**, but the crystalline solids were contaminated with $(Me_4N)(NO_3)$ salt, requiring copious washing with MeOH to obtain analytically pure samples. Finally, substitution of NO_3^- ions in the LnX_3 precursors by other inorganic ions, such as Cl^- or ClO_4^-, did not lead us to any crystalline material under various crystallization techniques and reaction conditions. It therefore seems that the presence of nitrates is essential for the stabilization and crystallization of the reported tetranuclear compounds. Compounds **1**–**7** are all stable and crystalline solids at room temperature and nonsensitive toward air and moisture. They are all soluble in MeCN, DMF, and DMSO and insoluble in almost all other organic solvents such as CH_2Cl_2, benzene, and toluene.

All complexes **1**–**7** have essentially the same IR spectra. Several bands appear in the ~1580–1390 cm^{-1} range, assigned to contributions from the stretching vibrations of the aromatic ring of $pdmH_2/pdmH^-$ ligands, which overlap with stretches of the nitrate bands.[38] The nitrate vibrations in the mull and KBr spectra of the representative complex **3** (also established by crystallography) are indicative of the simultaneous presence of ionic and coordinated NO_3^-. The former appears as a band at ~1388 cm^{-1} and is attributed to the $\nu_3(E')[\nu_d(NO)]$ mode of the D_{3h} ionic nitrate.[39] Bands at ~1423 and ~1321 cm^{-1} may be assigned to the $\nu_5(B_2)$ and $\nu_1(A_1)$ stretching modes (under C_{2v} symmetry), respectively, of the nitrato ligands; their separation is small (~102 cm^{-1}), in accordance with the monodentate character of two nitrate groups.[39]

Description of Structures. The structures of the reported complexes **1**–**7** are very similar, and thus, only the structure of representative complex **3** will be described in detail. The crystal structure of **3** consists of a $[Tb_4(NO_3)_2(pdmH)_6(pdmH_2)_2]^{4+}$ cation (Figure 1), four NO_3^- anions, and lattice MeOH

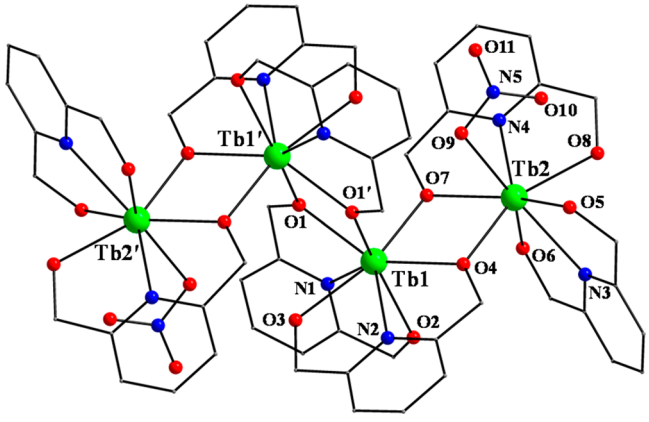

Figure 1. Partially labeled representation of the structure of the cation of **3**, with H atoms omitted for clarity. Primes are used for symmetry-related atoms; see the footnote of Table 2. Color code: Tb^{III} green, O red, N blue, C gray.

dx.doi.org/10.1021/ic5001045 | Inorg. Chem. 2014, 53, 3220–3229

molecules; the latter two will not be further discussed. Complex **3**·2MeOH crystallizes in the monoclinic space group $P2_1/n$ with the Tb_4 cation lying on an inversion center. Selected interatomic distances and angles are listed in Table 2.

Table 2. Selected Interatomic Distances (Angstroms) and Angles (degrees) for Complex 3[a]

Tb1–O1	2.324(3)	Tb2–O4	2.275(3)
Tb1–O1′	2.301(3)	Tb2–O5	2.424(4)
Tb1–O2	2.454(4)	Tb2–O6	2.395(4)
Tb1–O3	2.436(3)	Tb2–O7	2.301(3)
Tb1–O4	2.343(3)	Tb2–O8	2.447(4)
Tb1–O7	2.295(3)	Tb2–O9	2.495(4)
Tb1–N1	2.529(4)	Tb2–N3	2.542(4)
Tb1–N2	2.530(4)	Tb2–N4	2.491(4)
Tb1···Tb1′	3.771(6)	Tb2···Tb2′	9.357(9)
Tb1···Tb2	3.751(2)		
Tb1–O1–Tb1′	109.3(1)	Tb1–O7–Tb2	109.4(1)
Tb1–O4–Tb2	108.6(1)		

[a]Symmetry code: ′ = 1 − *x*, −*y*, −*z*.

The cation comprises a nonlinear, zigzag array of four Tb^{III} atoms (Tb2–Tb1–Tb1′ = 107.56°) with each Tb_2 pair bridged by the deprotonated alkoxido arms of two chelating/bridging $pdmH^-$ groups resulting in an overall $[Tb_4(\mu\text{-}OR)_6]^{6+}$ core (Figure 2). There is thus a total of six $\eta^1{:}\eta^1{:}\eta^2{:}\mu$ $pdmH^-$

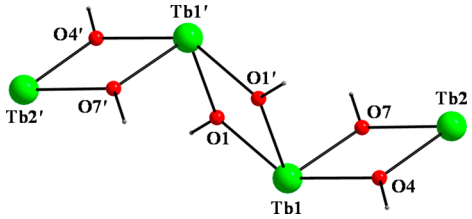

Figure 2. Labeled representation of the complete $[Tb_4(\mu\text{-}OR)_6]^{6+}$ core of **3**. Color scheme as in Figure 1.

groups, and peripheral ligation is completed by two neutral, tridentate (N,O,O) chelating $pdmH_2$ ligands and two monodentate NO_3^- groups, one each on the two extrinsic Tb^{III} atoms, Tb2 and Tb2′. The central Tb(1)–O(1)–Tb(1′)–O(1′) rhombus is strictly planar as a result of the inversion center, and the other two rhombs are nearly so, with the Tb(1)–O(4)–Tb(2)–O(7) torsion angle being only 0.8°. Tb^{III} atoms are both eight coordinate with distorted geometries.

To estimate the closer coordination polyhedra defined by the donor atoms around Tb1 and Tb2 in the asymmetric unit of **3**, a comparison of the experimental structural data with the theoretical data for the most common polyhedral structures with 8 vertices was performed by means of the program SHAPE.[40] Following the proposal by Avnir and co-workers[41] to consider symmetry and polyhedral shape as continuous properties that can be quantified from structural data, Alvarez and co-workers applied these concepts and the associated methodology to the stereochemical analysis of very large sets of molecular structures, including systems with 8-vertex polyhedra.[42] The so-called continuous shape measures (CShM) approach allows one to numerically evaluate by how much a particular structure deviates from an ideal shape.[43] There are many polyhedra with eight vertices such as Platonic solids (cube), Archimedean or Catalan (triakis tetrahedron) solids, and others such as triangular dodecahedra. In addition, prisms (biaugmented trigonal) or antiprisms (square antiprism) can be made with eight vertices as well as many semiregular three-dimensional figures. The most common of these, which will be considered here, are the octagon, the heptagonal pyramid, the hexagonal bipyramid, the triangular dodecahedron, and the four Johnson polyhedra (gyrobifastigium, elongated triangular bipyramid, biaugmented trigonal prism, and snub tetrahedron). The best fit (Table S1, Supporting Information) was obtained for the triangular dodecahedron (Tb1; Figure 3, left) and

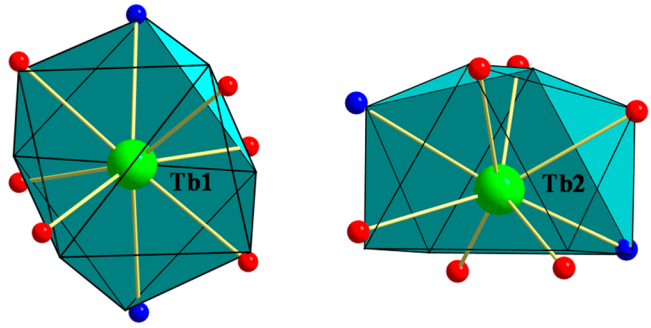

Figure 3. Triangular dodecahedron coordination sphere of Tb1 (left) and biaugmented trigonal prismatic geometry of Tb2 (right) in the structure of **3**. Points connected by the black lines define the vertices of the ideal polyhedron.

biaugmented trigonal prism (Tb2; Figure 3, right) with CShM values of 1.96 and 1.50, respectively. Values of CShM between 0.1 and 3 usually correspond to a not negligible but still small distortion from ideal geometry.[44]

Four distinct, and eight in total (including the symmetry related atoms), strong intramolecular hydrogen bonds are present in **3**·2MeOH. These include the protonated OH groups of the $pdmH_2/pdmH^-$ ligands, which act as donors, and an O atom from each monodentate or noncoordinated (counter-anion) NO_3^- group or the lattice solvate MeOH molecules as acceptors; their dimensions are O(3)···O(9′) 2.737(7) Å, H(3A)···O(9′) 1.918 Å, O(3)–H(3A)···O(9′) 161.9°; O(6)···O(12) 2.712(7) Å, H(6A)···O(12) 1.868 Å, O(6)–H(6A)···O(12) 175.2°; O(8)···O(15) 2.762(7) Å, H(8A)···O(15) 2.044 Å, O(8)–H(8A)···O(15) 142.2°; O(2)···O(18) 2.635(7) Å, H(2A)···O(18) 1.790 Å, O(2)–H(2A)···O(18) 175.4°. There are no significant intermolecular interactions, only weak contacts which serve to hold the molecules together in the crystal.

The Ln–N and Ln–O bond distances in **1**–**7** fall into the expected range for similar compounds and take shorter values as we move from **1** to **7**, which are consistent with the lanthanide contraction effect. There have been a large number of Ln_4 complexes reported in the literature, and these possess a wide variety of metal topologies such as linear,[45] rectangles,[46] squares and grids,[47] rhombs and butterflies,[48] cubanes,[49] and dimers of dimers.[50] However, complexes **1**–**7** join only a handful of previous Ln_4 compounds with a similar kind of extended, chain-like topology and an $[Ln_4(\mu\text{-}OR)_6]^{6+}$ core.[25,51]

Static Magnetic Properties. Variable-temperature direct current (dc) magnetic susceptibility studies were carried out on freshly prepared, crystalline samples of the potentially most interesting—from a magnetism viewpoint—complexes **2**·2MeOH, **3**·2MeOH, **4**, **5**, and **7** in the temperature range 5.0–300 K under an applied field of 0.1 T. Theoretically, the

dx.doi.org/10.1021/ic5001045 | Inorg. Chem. 2014, 53, 3220–3229

Eu^{III}_4 analogue (**1**) should not exhibit any magnetic moment, since Eu^{III} has an $^7F_0$ with $J = 0$, although some contribution from thermally accessible levels such as $^7F_1$ and $^7F_2$ may appear.[16,20b] The obtained data for all studied compounds are shown as $\chi_M T$ vs T plots in Figures 4 and 5. The experimental

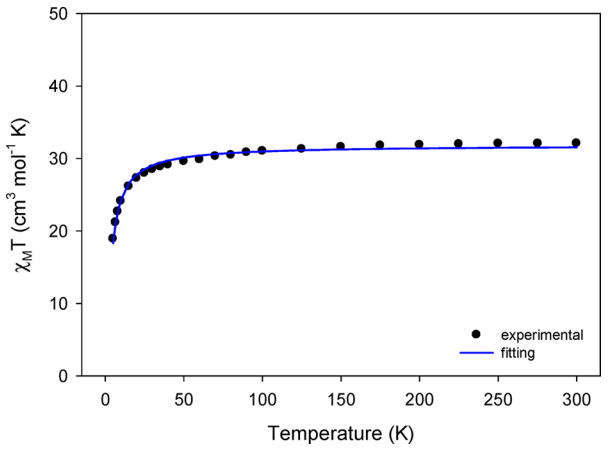

Figure 4. Temperature dependence of the $\chi_M T$ for **2**·2MeOH. Blue solid line is the fit of the data; see text for the fit parameters.

$\chi_M T$ values at room temperature in all cases are in very good agreement with the theoretical ones (31.50 cm^3 K mol^{-1} for **2**; 47.28 cm^3 K mol^{-1} for **3**; 56.68 cm^3 K mol^{-1} for **4**; 56.28 cm^3 K mol^{-1} for **5**; 10.28 cm^3 K mol^{-1} for **7**) for four noninteracting Gd^{III} ($^8S_{7/2}$, $S = 7/2$, $L = 0$, $g = 2$), Tb^{III} ($^7F_6$, $S = 3$, $L = 3$, $g = 3/2$), Dy^{III} ($^6H_{15/2}$, $S = 5/2$, $L = 5$, $g = 4/3$), Ho^{III} ($^5I_8$, $S = 2$, $L = 6$, $g = 5/4$), and Yb^{III} ($^2F_{7/2}$, $S = 1/2$, $L = 3$, $g = 8/7$) ions.[55]

For the isotropic Gd^{III}_4 (**2**·2MeOH) complex, the $\chi_M T$ product remains almost constant at a value of ∼31.4 cm^3 K mol^{-1} from 300 to ∼100 K and then steadily decreases to a minimum value of 18.31 cm^3 K mol^{-1} at 5.0 K (Figure 4). This is indicative of the presence of intramolecular antiferromagnetic exchange interactions between the four Gd^{III} centers and/or zero-field splitting effects.[48,49] The temperature-independent behavior (300−100 K) suggests that the coupling between the Gd^{III} ions is very weak as has been seen in many polynuclear Gd^{III} complexes.[45−50] Given the lack of any first-order orbital momentum for the Gd^{III} ions, we undertook the challenge to quantify the strength of the intramolecular magnetic exchange interactions in **2**·2MeOH. The tetranuclear compound was modeled with the spin Hamiltonian shown in eq 2.

$$\mathcal{H} = -2J(\hat{S}_1\cdot\hat{S}_2 + \hat{S}_1\cdot\hat{S}_{1'} + \hat{S}_{1'}\cdot\hat{S}_{2'}) \quad (2)$$

Data were fit using the program MAGMUN[52] by applying a simple $1 - J$ model. The fit (solid blue line in Figure 4) gave fit parameter values of $J = -0.09(1)$ cm^{-1} and $g = 2.00(1)$, in excellent agreement with the J values reported for antiferromagnetically coupled Gd^{III}_4 clusters of similar or slightly different metal topologies.[47−49] A fit of the data to a $2 - J$ model ($J_{11'} \neq J_{12}$ with $J_{12} = J_{1'2'}$ due to the molecular symmetry) gave results of comparable quality, but these might lead to overparametarization problems and have thus been ignored.

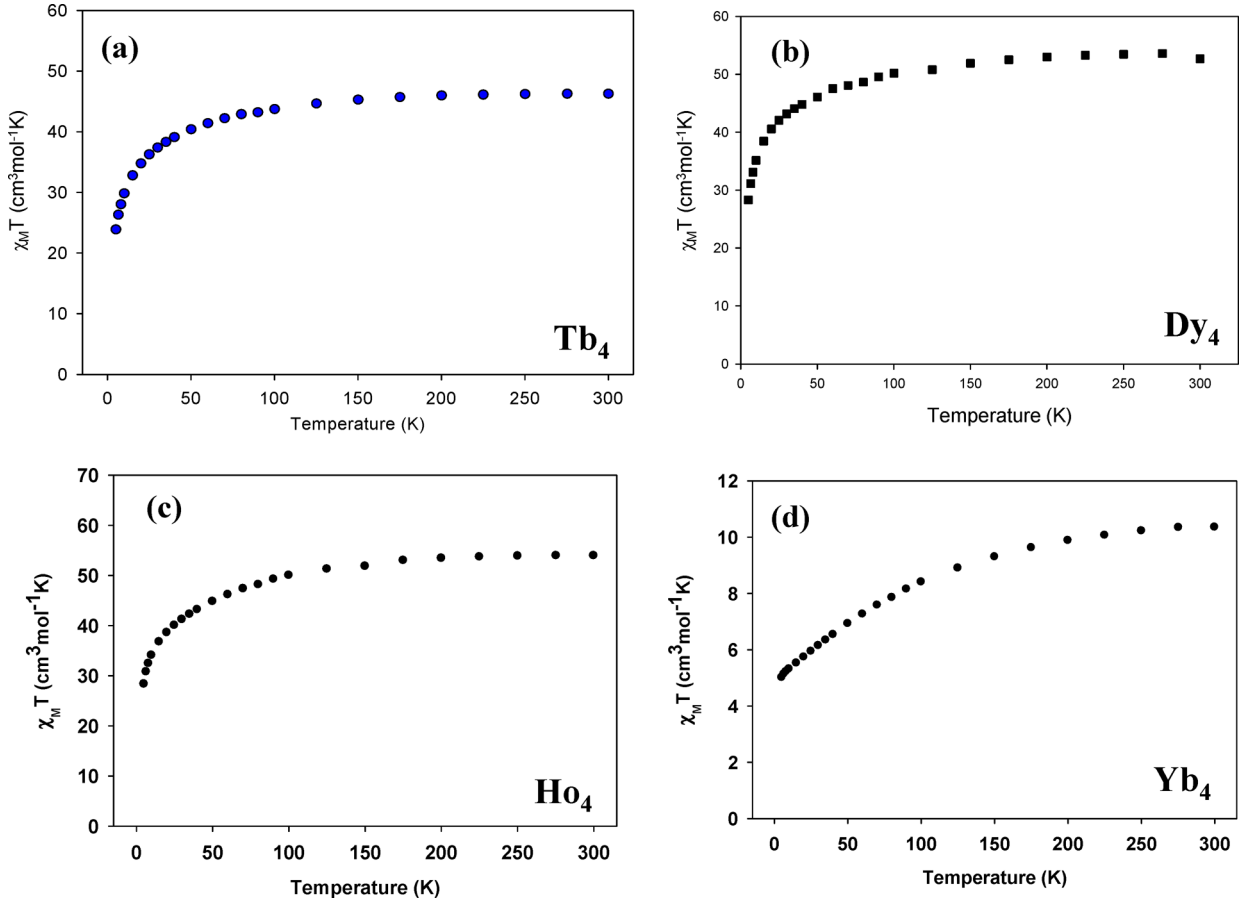

Figure 5. Plots of $\chi_M T$ *vs* T for complexes **3**·2MeOH (a), **4** (b), **5** (c), and **7** (d).

dx.doi.org/10.1021/ic5001045 | *Inorg. Chem.* 2014, 53, 3220−3229

For the anisotropic Tb^{III}_4 (**3**·2MeOH), Dy^{III}_4 (**4**), and Ho^{III}_4 (**5**) complexes, the thermal evolution of the magnetic susceptibility is very similar (Figure 5a, 5b, and 5c, respectively), in which the $\chi_M T$ product remains constant at a value of ∼46.3 (**3**), ∼53.5 (**4**), and ∼53.0 (**5**) cm^3 K mol^{-1} from 300 to ∼150 K and then steadily decreases to a minimum value of 23.88 (**3**), 28.75 (**4**), and 28.33 (**5**) cm^3 K mol^{-1} at 5.0 K. Such low-temperature decrease of the $\chi_M T$ product is mainly due to depopulation of the excited Stark sublevels of the Ln^{III} ions and the probable weak antiferromagnetic interactions between the metal centers which unfortunately cannot be quantified due to the strong orbital momentum of these Ln^{III} ions.[8] For the Yb^{III}_4 (**7**) complex, the $\chi_M T$ product starts to decrease steadily from a value of 10.35 cm^3 K mol^{-1} at 300 K to a minimum value of 5.01 cm^3 K mol^{-1} at 5.0 K (Figure 5d). Such gradual decrease upon cooling can be ascribed to the thermal depopulation of the ligand field levels.[53] These ligand field levels result from the crystal field created in the first approximation by point charges in the coordination sphere of the lanthanide and constitute linear combinations of M_J's components of the total kinetic moment and depend on the site symmetry.[54]

The field dependence of magnetization studies at low temperatures does not show any irregular features for all complexes other than the expected ones for polynuclear, weakly coupled lanthanide(III) clusters. Briefly, the lack of true saturation in magnetization of complexes **3**, **4**, **5**, and **7** indicates the presence of some magnetic anisotropy and/or population of low-lying excited states.[45−50] In the case of isotropic complex **2**, the magnetization almost reaches a saturation of 28.0 μ_B at the highest fields, which is in good agreement with the expected value for four noncoupled Gd^{III} ions (7.0 μ_B per Gd^{III}). This further supports the weak nature of the magnetic exchange interactions between the Gd^{III} centers, so that the antiferromagnetic interactions are easily overcome by the external field.[8,55] The slight deviation of M vs H/T for **2** at different low temperatures (<10 K) and small magnetic fields (0.1−1.0 T) is due to the population of low-lying excited states with S larger than the ground state (Figure S1, left, Supporting Information). This is also supported by the continuous decrease of the in-phase, $\chi'_M T$, product as the temperature decreases down to 1.8 K (Figure S1, right, Supporting Information).

Dynamic Magnetic Properties. In light of the conclusions deduced by the static magnetic measurements on all reported compounds, alternating current magnetic susceptibility studies have been also carried out in order to investigate the magnetization dynamics of the anisotropic Tb^{III}_4 (**3**), Dy^{III}_4 (**4**), Ho^{III}_4 (**5**), and Yb^{III}_4 (**7**) clusters under a zero dc magnetic field. Alternating current studies were performed in the 1.8−15 K range using a 3.5 G ac field oscillating at frequencies in the 50−1000 Hz range. If the barrier to magnetization relaxation is significant compared to thermal energy (kT) then there is a nonzero χ''_M signal which will be also frequency dependent. Such frequency-dependent χ''_M signals are indicative of the superparamagnetic-like properties of a SMM (but they do not prove the presence of a SMM[56]). For fast relaxing SMMs and/or SMMs with a strong quantum tunneling rate an entirely visible peak of the χ''_M signal is not often observed even at the lowest possible temperature (∼1.8 K) of any commercial SQUID magnetometer; only the tails of peak maxima can thus be detected. This is usually the case for high-nuclearity lanthanide SMMs.

Complex **4** is the only member of this family of tetranuclear clusters which shows frequency-dependent out-of-phase χ''_M tails of signals at temperatures below ∼5 K (Figure 6),

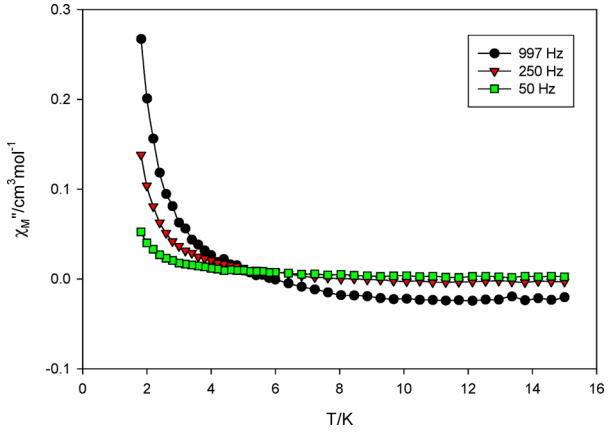

Figure 6. Out-of-phase (χ''_M) vs T ac susceptibility signals for **4** in a 3.5 G field oscillating at the indicated frequencies. The decrease in the χ''_M signal in the 6−15 K range at 997 Hz is an instrumentation artifact.[57]

indicative of the slow magnetization relaxation of an SMM with a small energy barrier for magnetization reversal. Such behavior most likely arises from predominant single-ion effects of the individual Dy^{III} centers within **4**.[8,25,45−51] There were no out-of-phase ac signals down to 1.8 K for the remaining compounds (Figure S2, Supporting Information). Thus, it can be tentatively seen that while **4** shows slow magnetization relaxation the isostructural complex **3** does not. This difference most likely originates from the fact that Dy^{III} is a Kramer ion, and irrespective of the ligand field it is expected to possess a bistable ground state. On the other hand, Tb^{III} is a non-Kramer ion, and so its complexes will have a bistable ground state only if it has an axially symmetric ligand field.[8,50d] Efforts to obtain more relaxation data and observe maxima by applying an external dc field led only to a slight enhancement of the out-of-phase signal without improving the chances to calculate an energy barrier.

Photoluminescence Studies. In order to gain any possible access into additional physical properties for this family of tetranuclear 4f-metal complexes, we decided to perform photoluminescence studies on the Eu^{III}_4 (**1**), Tb^{III}_4 (**3**·2MeOH), and Dy^{III}_4 (**4**) analogues in the solid state and at room temperature (Figure 7). The free ligand $pdmH_2$ does not emit in the solid state or in solution.[58] However, it has been shown[58] that $pdmH_2$ could potentially act as a good "antenna" ligand for enhancement of luminescence in a Zn^{II}_6 cluster. The

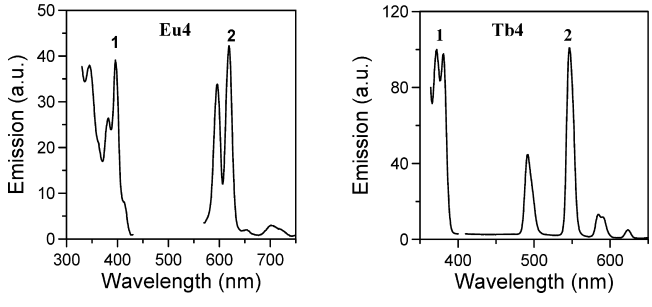

Figure 7. Excitation (1) and emission (2) spectra of solid complexes **1** (left) and **3** (right) at room temperature.

dx.doi.org/10.1021/ic5001045 | Inorg. Chem. 2014, 53, 3220−3229

origin of emission in that Zn^{II}_6 compound is still uncertain due to the copresence of aromatic benzoate bridging ligands which also affect the resulting optical response.

The Eu^{III}_4 and Tb^{III}_4 complexes show sharp and narrow emission bands arising from the characteristic 4f → 4f transitions.[2,16,19,20] However, the Dy^{III}_4 analogue does not display the expected spectrum for a Dy^{III} emission, with the characteristic peaks located at ~480 ($^4F_{9/2} \rightarrow {}^6H_{15/2}$) and ~575 nm ($^4F_{9/2} \rightarrow {}^6H_{13/2}$). This is likely due to a significant quenching of the emission intensity for **4** due to paramagnetic effects.[59] Upon maximum excitation at 396 nm, the solid-state emission spectrum of **1** displays relatively strong red photoluminescence, assigned to the characteristic $^5D_0 \rightarrow {}^7F_J$ (J = 0−4) transitions of Eu^{3+}. Specific assignments are as follows: $^5D_0 \rightarrow {}^7F_{0,1}$ (596 nm), $^5D_0 \rightarrow {}^7F_2$ (619 nm), $^5D_0 \rightarrow {}^7F_3$ (655 nm), and $^5D_0 \rightarrow {}^7F_4$ (702 nm).[16,20b,21] For complex **3**, upon excitation at 380 nm, a strong green luminescence emission has been obtained which can be ascribed to the characteristic $^5D_4 \rightarrow {}^7F_J$ (J = 3; 623 nm, J = 4; 585 nm, J = 5; 547 nm, J = 6; 492 nm) transitions of Tb^{III}.[16,21,47c] In cases of **1** and **3**, the emission results demonstrate the ability of the $pdmH_2$ ligand to act as an efficient "antenna" group by transferring energy to the Ln^{III} emission states and preventing back-transfer processes from the 4f-metal ions, which would otherwise quench or vanish the obtained emission.

CONCLUSIONS

Our longstanding interest in the systematic investigation of pyridine-2,6-dimethanol ($pdmH_2$) as a bridging/chelating ligand for synthesis of polynuclear metal complexes with interesting either magnetic properties or photoluminescence behaviors has been well documented over the last 10 years through isolation of several high-spin 3d metal clusters and SMMs[24] or Zn^{II}-based complexes[58] with emission characteristics. Very recently, we were able to show that $pdmH_2$ can also lead to unprecedented, very high nuclearity 3d/4f-metal clusters with the reported $Cu^{II}_{15}Gd^{III}_7$ compound exhibiting low-temperature magnetocaloric effect.[60] We have now brought together molecular magnetism and optics via employment of $pdmH_2$ in homometallic lanthanide(III) coordination chemistry. In particular, we reported a seven-membered family of tetranuclear $[Ln^{III}_4(NO_3)_2(pdmH)_6(pdmH_2)_2](NO_3)_4$ complexes with different 4f-metal ions and a rare zigzag topology. The Dy^{III}_4 analogue shows slow relaxation of magnetization at low temperatures, whereas the Eu^{III}_4 and Tb^{III}_4 compounds exhibit intense red and green photoluminescence in the visible region, respectively. The magnetic susceptibility studies of the isotropic Gd^{III}_4 analogue allowed us to quantitatively determine the nature and strength of the magnetic exchange interactions between the four spin carriers, which were found to be antiferromagnetic and very weak (J = −0.09 cm^{-1} for Gd^{III}_4), as is almost always the case in Ln(III) complexes due to the radially contracted nature of 4f orbitals.[8,55]

We are currently pursuing higher nuclearity 4f-metal complexes with the doubly deprotonated form of the $pdmH_2$ ligand and in the presence of various ancillary inorganic groups with bridging affinity, such as N_3^-, NCO^-, and CO_3^{2-}. Finally, it is that specific non-well-behaved nature of the polyalkoxide ligands which makes (in general) metal cluster chemistry totally unpredictable and one of the most intriguing areas of modern coordination chemistry.

ASSOCIATED CONTENT

Supporting Information

Crystallographic data for **3**·2MeOH, **5**·2MeOH, **6**·2MeOH, and **7**·2MeOH in CIF formas, CShM values for different coordination polyhedra, and various magnetism plots. This material is available free of charge via the Internet at http://pubs.acs.org.

AUTHOR INFORMATION

Corresponding Author

*E-mail: tstamatatos@brocku.ca.

Notes

The authors declare no competing financial interest.

ACKNOWLEDGMENTS

We thank the Ontario Trillium Foundation (graduate scholarship to D.I.A), NSERC Discovery Grant and CFI (to Th.C.S), the Fundação para a Ciência e a Tecnologia (FCT, MEC, Portugal) for financial support under the strategic project Pest-C/EQB/LA0006/2011 (to REQUIMTE), and the National Science Foundation (DMR-1213030 to G.C) for funding. V.B. acknowledges financial support by the European Union (European Social Fund, ESF) and Greek national funds through the Operational Program "Education and Lifelong Learning" of the National Strategic Reference Framework (NSRF)-Research Funding Program: Archimedes III.

REFERENCES

(1) (a) Murugesu, M. *Nat. Chem.* **2012**, *4*, 347−348. (b) Eliseeva, S. V.; Bünzli, J.-C. G. *New J. Chem.* **2011**, *35*, 1165−1176. (c) Ganzhorn, M.; Klyatskaya, S.; Ruben, M.; Wernsdorfer, W. *Nat. Nanotechnol.* **2013**, *8*, 165−169.

(2) (a) Bünzli, J.-C. G.; Eliseeva, S. V. *Chem. Sci.* **2013**, 1939−1949. (b) Kelkar, S. S.; Reineke, T. M. *Bioconjugate Chem.* **2011**, *22*, 1879−1903. (c) Bünzli, J.-C. G.; Eliseeva, S. V. *Basics of Lanthanide Photophysics: Springer Series on Fluorescence*; 2011; Vol. *7*, pp 1−45. (d) Shibasaki, M.; Yoshikawa, M. *Chem. Rev.* **2002**, *102*, 2187−2210.

(3) For an in-depth discussion on the various meanings of the term "cluster" in several areas of inorganic chemistry, see: (a) Chisholm, M. H. *Polyhedron* **1998**, *17*, 2773−2774. (b) Fielden, J.; Cronin, L. *Encyclopedia of Supermolecular Chemistry*: DOI: 10.1081/E-ESMC-120024346.

(4) (a) Simuneková, M.; Prodius, D.; Mereacre, V.; Schwendt, P.; Turta, C.; Bettinelli, M.; Speghini, A.; Lan, Y.; Anson, C. E.; Powell, A. K. *RSC Adv.* **2013**, *3*, 6299−6304. (b) Wang, B.; Jiang, S.; Wang, X.; Gao, S. In *Rare Earth Coordination Chemistry: Fundamentals and Applications*; Huang, C.-H., Ed.; Wiley: New York, 2010; pp 355−407.

(5) For example, see: Zheng, Y.; Zhang, Q.-C.; Long, L.-S.; Huang, R.-B.; Müller, A.; Schnack, J.; Zheng, L.-S.; Zheng, Z. *Chem. Commun.* **2013**, *49*, 36−38.

(6) For example, see: Moreno Pineda, E.; Tuna, F.; Pritchard, R. G.; Regan, A. C.; Winpenny, R. E. P.; McInnes, A. J. L. *Chem. Commun.* **2013**, *49*, 3522−3524.

(7) Christou, G. *Polyhedron* **2005**, *24*, 2065−2075.

(8) (a) Woodruff, D. N.; Winpenny, R. E. P.; Layfield, R. A. *Chem. Rev.* **2013**, *113*, 5110−5148. (b) Rinehart, J. D.; Long, J. R. *Chem. Sci.* **2011**, *2*, 2078−2085. (c) Sorace, L.; Benelli, C.; Gatteschi, D. *Chem. Soc. Rev.* **2011**, *40*, 3092−3104. (d) Guo, Y. N.; Xu, G. F.; Guo, Y.; Tang, J. *Dalton Trans.* **2011**, *40*, 9953−9963. (e) Sessoli, R.; Powell, A. K. *Coord. Chem. Rev.* **2009**, *253*, 2328−2341. (f) Wang, B. W.; Jiang, S. D.; Wang, X. T.; Gao, S. *Sci. China, Ser. B: Chem.* **2009**, *52*, 1739−1759. (g) Brooker, S.; Kitchen, J. A. *Dalton Trans.* **2009**, 7331−7340. (h) Habib, F.; Murugesu, M. *Chem. Soc. Rev.* **2013**, *42*, 3278−3288.

(9) (a) Evangelisti, M.; Luis, F.; de Jongh, L. J.; Affronte, M. *J. Mater. Chem.* **2006**, *16*, 2534−2549. (b) Evangelisti, M.; Brechin, E. K. *Dalton*

Trans. **2010**, *39*, 4672−4676. (c) Evangelisti, M.; Roubeau, O.; Palacios, E.; Camón, A.; Hooper, T. N.; Brechin, E. K.; Alonso, J. J. *Angew. Chem., Int. Ed.* **2011**, *50*, 6606−6609. (d) Chang, L.-X.; Xiong, G.; Wang, L.; Cheng, P.; Zhao, B. *Chem. Commun.* **2013**, *49*, 1055−1057.

(10) (a) Guo, P.-H.; Liu, J.-L.; Jia, J.-H.; Wang, J.; Guo, F.-S.; Chen, Y.-C.; Lin, W.-Q.; Leng, J.-D.; Bao, D.-H.; Zhang, X.-D.; Luo, J.-H.; Tong, M.-L. *Chem.—Eur. J.* **2013**, *19*, 8769−8773 and references cited therein. (b) Gatteschi, D.; Sessoli, R.; Villain, J. *Molecular Nanomagnets*; Oxford University Press: New York, 2007.

(11) For some representative examples, see: (a) Ishikawa, N.; Sugita, M.; Ishikawa, T.; Koshihara, S.; Kaizu, Y. *J. Am. Chem. Soc.* **2003**, *125*, 8694−8695. (b) Cucinotta, G.; Perfetti, M.; Luzon, J.; Etienne, M.; Car, P. E.; Caneschi, A.; Calvez, G.; Bernot, K.; Sessoli, R. *Angew. Chem., Int. Ed.* **2012**, *51*, 1606−1610. (c) Boulon, M. E.; Cucinotta, G.; Luzon, J.; Degl'Innocenti, C.; Perfetti, M.; Bernot, K.; Calvez, G.; Caneschi, A.; Sessoli, R. *Angew. Chem., Int. Ed.* **2013**, *52*, 350−354. (d) Rinehart, J. D.; Fang, M.; Evans, W. J.; Long, J. R. *Nat. Chem.* **2011**, *3*, 538−542. (e) Rinehart, J. D.; Fang, M.; Evans, W. J.; Long, J. R. *J. Am. Chem. Soc.* **2011**, *133*, 14236−14239. (f) Long, J.; Habib, F.; Lin, P. H.; Korobkov, I.; Enright, G.; Ungur, L.; Wernsdorfer, W.; Chibotaru, L. F.; Murugesu, M. *J. Am. Chem. Soc.* **2011**, *133*, 5319−5328. (g) Tang, J.; Hewitt, I.; Madhu, N. T.; Chastanet, G.; Wernsdorfer, W.; Anson, C. E.; Benelli, C.; Sessoli, R.; Powell, A. K. *Angew. Chem., Int. Ed.* **2006**, *45*, 1729−1733. (h) Blagg, R. J.; Muryn, C. A.; McInnes, E. J. L.; Tuna, F.; Winpenny, R. E. P. *Angew. Chem., Int. Ed.* **2011**, *50*, 6530−6533. (i) Blagg, R. J.; Ungur, L.; Tuna, F.; Speak, J.; Comar, P.; Collison, D.; Wernsdorfer, W.; McInnes, E. J. L.; Chibotaru, L.; Winpenny, R. E. P. *Nat. Chem.* **2013**, *5*, 673−678.

(12) (a) Friedman, J. R.; Sarachik, M. P. *Phys. Rev. Lett.* **1996**, *76*, 3830−3833. (b) Thomas, L.; Lionti, L.; Ballou, R.; Gatteschi, D.; Sessoli, R.; Barbara, B. *Nature* **1996**, *383*, 145−147.

(13) (a) Wernsdorfer, W.; Sessoli, R. *Science* **2000**, 2417. (b) Wernsdorfer, W.; Soler, M.; Christou, G.; Hendrickson, D. N. *J. Appl. Phys.* **2002**, *91*, 7164−7166. (c) Wernsdorfer, W.; Chakov, N. E.; Christou, G. *Phys. Rev. Lett.* **2005**, *95*, 037203 (1−4).

(14) (a) Bogani, L.; Wernsdorfer, W. *Nat. Mater.* **2008**, *7*, 179−186. (b) Vincent, R.; Klyatskaya, S.; Ruben, M.; Wernsdorfer, W.; Balestro, F. *Nature* **2012**, *488*, 357−360. (c) Urdampilleta, M.; Klyatskaya, S.; Cleuziou, J.-P.; Ruben, M.; Wernsdorfer, W. *Nat. Mater.* **2011**, *10*, 502−506.

(15) For example, see: Silver, J. In *Comprehensive Coordination Chemistry II*; McCleverty, J. A., Meyer, T. J., Eds.; Elsevier: Amsterdam, 2004; Vol. *9*, p 689.

(16) Cotton, S. *Lanthanide and Actinide Chemistry*; John Wiley & Sons: West Sussex, 2006.

(17) (a) Biju, S.; Gopakumar, N.; Bünzli, J.-C. G.; Scopelliti, R.; Kim, H. K.; Reddy, M. L. P. *Inorg. Chem.* **2013**, *52*, 8750−8758. (b) Su, Q.; Pei, Z.; Chi, L.; Zhang, H.; Zhang, Z.; Zou, F. J. *Alloys Compd.* **1993**, *192*, 25−27. (c) Wei, K.; Machewirth, D. P.; Wenzel, J.; Snitzer, E.; Sigel, J. G. H. *Opt. Lett.* **1994**, *19*, 904−906.

(18) (a) Sabbatini, N.; Guardigli, M.; Lehn, J.-M. *Coord. Chem. Rev.* **1993**, *123*, 201−228. (b) Bünzli, J.-C. G.; Piguet, C. *Chem. Soc. Rev.* **2005**, *34*, 1048−1077.

(19) (a) Lehn, J.-M. *Angew. Chem., Int. Ed.* **1990**, *29*, 1304−1319. (b) Weissman, S. I. *J. Chem. Phys.* **1942**, *10*, 214−217. (c) Binnemans, K. *Chem. Rev.* **2009**, *109*, 4283−4374. (d) Bekiari, V.; Thiakou, K. A.; Raptopoulou, C. P.; Perlepes, S. P.; Lianos, P. *J. Lumin.* **2008**, *128*, 481−488.

(20) (a) Canaj, A. B.; Tzimopoulos, D. I.; Philippidis, A.; Kostakis, G. E.; Milios, C. J. *Inorg. Chem.* **2012**, *51*, 7451−7453. (b) Alexandropoulos, D. I.; Mukherjee, S.; Papatriantafyllopoulou, C.; Raptopoulou, C. P.; Psycharis, V.; Bekiari, V.; Christou, G.; Stamatatos, Th. C. *Inorg. Chem.* **2011**, *50*, 11276−11278. (c) Menelaou, M.; Ouharrou, F.; Rodríguez, L.; Roubeau, O.; Teat, S. J.; Aliaga-Alcalde, N. *Chem.—Eur. J.* **2012**, *18*, 11545−11549. (d) Yamashita, K.; Miyazaki, R.; Kataoka, Y.; Nakanishi, T.; Hasegawa, Y.; Nakano, M.; Yamamura, T.; Kajiwara, T. *Dalton Trans.* **2013**, *42*, 1987−1990. (e) Burrow, C. E.; Burchell, T. J.; Lin, P.-H.; Habib, F.; Wernsdorfer, W.; Clérac, R.; Murugesu, M. *Inorg. Chem.* **2009**, *48*, 8051−8053.

(21) (a) Magennis, S. W.; Parsons, S.; Pikramenou, Z. *Chem.—Eur. J.* **2003**, *8*, 5761−5771. (b) Mancino, G.; Ferguson, A. J.; Beeby, A.; Long, N. J.; Jones, T. S. *J. Am. Chem. Soc.* **2005**, *127*, 524−525.

(22) (a) Stamatatos, Th. C.; Christou, G. *Inorg. Chem.* **2009**, *48*, 3308−3322. and references therein (b) Stamatatos, Th. C.; Efthymiou, C. G.; Stoumpos, C. C.; Perlepes, S. P. *Eur. J. Inorg. Chem.* **2009**, 3361−3391. (Microreview) (c) Tasiopoulos, A. J.; Perlepes, S. P. *Dalton Trans.* **2008**, 5537−5555 (Perspective).

(23) (a) Milios, C. J.; Stamatatos, Th. C.; Perlepes, S. P. *Polyhedron* **2006**, *25*, 134−194. (b) Stamatatos, Th. C.; Foguet-Albiol, D.; Stoumpos, C. C.; Raptopoulou, C. P.; Terzis, A.; Wernsdorfer, W.; Perlepes, S. P.; Christou, G. *J. Am. Chem. Soc.* **2005**, *127*, 15380−15381. (c) Papatriantafyllopoulou, C.; Stamatatos, Th. C.; Efthymiou, C. G.; Cunha-Silva, L.; Almeida Paz, F. A.; Perlepes, S. P.; Christou, G. *Inorg. Chem.* **2010**, *49*, 9743−9745 and references therein..

(24) For some representative examples, see: (a) Stamatatos, Th. C.; Vlahopoulou, G. C.; Raptopoulou, C. P.; Terzis, A.; Escuer, A.; Perlepes, S. P. *Inorg. Chem.* **2009**, *48*, 4610−4612. (b) Taguchi, T.; Stamatatos, Th. C.; Abboud, K. A.; Jones, C. M.; Poole, K. M.; O' Brien, T. A.; Christou, G. *Inorg. Chem.* **2008**, *47*, 4095−4108. (c) Taguchi, T.; Thompson, M. S.; Abboud, K. A.; Christou, G. *Dalton Trans.* **2010**, *39*, 2131−2133. (d) Murugesu, M.; Habrych, M.; Wernsdorfer, W.; Abboud, K. A.; Christou, G. *J. Am. Chem. Soc.* **2004**, *126*, 4766−4767. (e) Stamatatos, Th. C.; Abboud, K. A.; Wernsdorfer, W.; Christou, G. *Angew. Chem., Int. Ed.* **2007**, *46*, 884−888. (f) Alexopoulou, K. I.; Raptopoulou, C. P.; Psycharis, V.; Terzis, A.; Tangoulis, V.; Stamatatos, Th. C.; Perlepes, S. P. *Aust. J. Chem.* **2012**, *65*, 1608−1619.

(25) (a) Yang, P.-P.; Gao, X.-F.; Song, H.-B.; Zhang, S.; Mei, X.-L.; Li, L.-C.; Liao, D.-Z. *Inorg. Chem.* **2011**, *50*, 720−722. (b) Yang, P.-P. *Z. Anorg. Allg. Chem.* **2011**, *637*, 1234−1237.

(26) Kottke, T.; Stalke, D. *J. Appl. Crystallogr.* **1993**, *26*, 615−619.

(27) *APEX2, Data Collection Software*, Version 2.1-RC13l Bruker AXS: Delft, The Netherlands, 2006.

(28) *Cryopad, Remote Monitoring and Control*, Version 1.451, *Oxford Cryosystems*, Oxford, 2006.

(29) *SAINT+, Data Integration Engine*, v. 7.23a; Bruker AXS: 1997−2005.

(30) Sheldrick, G. M. *SADABS v.2.01, Bruker/Siemens Area Detector Absorption Correction Program*; Bruker AXS: 1998.

(31) Sheldrick, G. M. *SHELXS-97, Program for Crystal Structure Solution*; University of Göttingen: Göttingen, 1997.

(32) Sheldrick, G. M. *Acta Crystallogr., Sect. A* **2008**, *64*, 112−122.

(33) Sheldrick, G. M. *SHELXL-97, Program for Crystal Structure Refinement*; University of Göttingen: Göttingen, 1997.

(34) Mercury; Bruno, I. J.; Cole, J. C.; Edgington, P. R.; Kessler, M. K.; Macrae, C. F.; McCabe, P.; Pearson, J.; Taylor, R. *Acta Crystallogr., Sect. B* **2002**, *58*, 389−397.

(35) Bradenburg, K. *DIAMOND, Release 3.1f*; Crystal Impact GbR: Bonn, Germany, 2008.

(36) Bain, G. A.; Berry, J. F. *J. Chem. Educ.* **2008**, *85*, 532−536.

(37) Representative references: (a) Hewitt, I. J.; Tang, J.; Madhu, N. T.; Anson, C. E.; Lan, Y.; Luzon, J.; Etienne, M.; Sessoli, R.; Powell, A. K. *Angew. Chem., Int. Ed.* **2010**, *49*, 6352−6356. (b) Xue, S.; Zhao, L.; Guo, Y. N.; Chen, X. H.; Tang, J. *Chem. Commun.* **2012**, *48*, 7031−7033. (c) Langley, S. K.; Moubaraki, B.; Murray, K. S. *Polyhedron* **2013**, *64*, 255−261. (d) Langley, S. K.; Moubaraki, B.; Murray, K. S. *Inorg. Chem.* **2012**, *51*, 3947−3949. (e) Sharples, J. W.; Zheng, Y.; Tuna, F.; McInnes, E. J. L.; Collison, D. *Chem. Commun.* **2011**, *47*, 7650−7652. (f) Tian, H.; Zhao, L.; Guo, Y. N.; Guo, Y.; Tang, J.; Liu, Z. *Chem. Commun.* **2012**, *48*, 708−710. (g) Miao, Y. L.; Liu, J. L.; Li, J. Y.; Leng, J. D.; Ou, Y. C.; Tong, M. L. *Dalton Trans.* **2011**, *40*, 10229−1236. (h) Miao, Y. L.; Liu, J. L.; Leng, J. D.; Lina, Z. J.; Tong, M. L. *Cryst. Eng. Commun.* **2011**, *13*, 3345−3348.

(38) Vlahopoulou, G. V.; Alexandropoulos, D. I.; Raptopoulou, C. P.; Perlepes, S. P.; Escuer, A.; Stamatatos, Th. C. *Polyhedron* **2009**, *28*, 3235−3242.

(39) (a) Nakamoto, K. *Infrared and Raman Spectra of Inorganic and Coordination Compounds*, 4th Ed.; Wiley: New York, 1986; pp 229, 254−257. (b) Katsoulakou, E.; Bekiari, V.; Raptopoulou, C. P.; Terzis, A.; Lianos, P.; Manessi-Zoupa, E.; Perlepes, S. P. *Spectrochim. Acta A* **2005**, *61*, 1627−1638.
(40) Llunell, M.; Casanova, D.; Girera, J.; Alemany, P.; Alvarez, S. *SHAPE*, version 2.0; Barcelona, Spain, 2010.
(41) Zabrodsky, H.; Peleg, S.; Avnir, D. *J. Am. Chem. Soc.* **1992**, *114*, 7843−7851.
(42) Ruiz-Martinez, A.; Casanova, D.; Alvarez, S. *Chem.—Eur. J.* **2008**, *14*, 1291−1303.
(43) Zabrodsky, H.; Peleg, S.; Avnir, D. *J. Am. Chem. Soc.* **1993**, *115*, 8278−8289.
(44) Alvarez, S.; Alemany, P.; Casanova, D.; Cirera, J.; Llunell, M.; Avnir, D. *Coord. Chem. Rev.* **2005**, *249*, 1693−1708.
(45) (a) Guo, Y.-N.; Xu, G.-F.; Gamez, P.; Zhao, L.; Lin, S.-Y.; Deng, R.; Tang, J.; Zhang, H.-J. *J. Am. Chem. Soc.* **2010**, *132*, 8538−8539. (b) Yang, X.; Chan, C.; Lam, D.; Schipper, D.; Stanley, J. M.; Chen, X.; Jones, R. A.; Holiday, B. J.; Wong, W.-K.; Chen, S.; Chen, Q. *Dalton Trans.* **2012**, *41*, 11449−11453. (c) Lin, S.-Y.; Zhao, L.; Ke, H.; Guo, Y.-N.; Tang, J.; Dou, J. *Dalton Trans.* **2012**, *41*, 3248−3252. (d) Ke, H.; Xu, G.-F.; Guo, Y.-N.; Gamez, P.; Beavers, C. M.; Teat, S. J.; Tang, J. *Chem. Commun.* **2010**, *46*, 6057−6059. (e) Yang, X.; Jones, R. A.; Wong, W.-K. *Chem. Commun.* **2008**, 3266−3268.
(46) (a) Franklin, S. J.; Raymond, K. N. *Inorg. Chem.* **1994**, *33*, 5794−5804. (b) Miyashita, Y.; Sanada, M.; Islam, M. M.; Amir, N.; Koyano, T.; Ikeda, H.; Fujisawa, K.; Okamoto, K. *Inorg. Chem. Commun.* **2005**, *8*, 785−803. (c) Ronson, T. K.; Adams, H.; Harding, L. P.; Pope, S. J. A.; Sykes, D.; Faulkner, S.; Ward, M. D. *Dalton Trans.* **2007**, 1006−1022. (d) Boyle, T. J.; Ottley, L. A. M.; Daniel-Taylor, S. D.; Tribby, L. J.; Bunge, S. D.; Costello, A. L.; Alam, T. M.; Gordon, J. C.; McCleskey, T. M. *Inorg. Chem.* **2007**, *46*, 3705−3713. (e) Regueiro-Figueroa, M.; Esteban-Gomez, D.; de Blas, A.; Rodriguez-Blas, T.; Platas-Iglesias, C. *Eur. J. Inorg. Chem.* **2010**, 3586−3595.
(47) For representative references, see: (a) Xue, S.; Zhao, L.; Guo, Y.-N.; Tang, J. *Dalton Trans.* **2012**, *41*, 351−353. (b) Coles, M. P.; Hitchcock, P. B.; Khvostov, A. V.; Lappert, M. F.; Li, Z.; Protchenko, A. V. *Dalton Trans.* **2010**, *39*, 6780−6788. (c) Bi, Y.; Wang, X.-T.; Liao, W.; Wang, X.; Deng, R.; Zhang, H.; Gao, S. *Inorg. Chem.* **2009**, *48*, 11743−11747. (d) Bilyk, A.; Dunlop, J. W.; Fuller, R. O.; Hall, A. K.; Harrowfield, J. M.; Hosseini, M. W.; Koutsantonis, G. A.; Murray, I. W.; Skelton, B. W.; Sobolev, A. N.; Stamps, R. L.; White, A. H. *Eur. J. Inorg. Chem.* **2010**, 2127−2152. (e) Anwar, M. U.; Thompson, L. K.; Dave, L. N.; Habib, F.; Murugesu, M. *Chem. Commun.* **2012**, *48*, 4576−4578. (f) Randell, N. M.; Anwar, M. U.; Drover, M. W.; Dawe, L. N.; Thompson, L. K. *Inorg. Chem.* **2013**, *52*, 6731−6742.
(48) (a) Guo, P.-H.; Lui, J.-L.; Zhang, Z.-M.; Ungur, L.; Chibotaru, L. F.; Leng, J.-D.; Guo, F.-S.; Tong, M.-L. *Inorg. Chem.* **2012**, *51*, 1233−1235. (b) Thompson, M. K.; Lough, A. J.; White, A. J. P.; Williams, D. J.; Kahwa, I. A. *Inorg. Chem.* **2003**, *42*, 4828−4841. (c) Yan, P.-F.; Lin, P.-H.; Habib, F.; Aharen, T.; Murugesu, M.; Deng, Z.-P.; Li, G.-M.; Sun, W.-B. *Inorg. Chem.* **2011**, *50*, 7059−7065. (d) Abbas, G.; Lan, Y.; Kostakis, G. E.; Wernsdorfer, W.; Anson, C. E.; Powell, A. K. *Inorg. Chem.* **2010**, *49*, 8067−8072. (e) Xue, S.; Zhao, L.; Guo, Y.-N.; Deng, R.; Guo, Y.; Tang, J. *Dalton Trans.* **2011**, *40*, 8347−8352. (f) Zheng, Y.-Z.; Lan, Y.; Anson, C. E.; Powell, A. K. *Inorg. Chem.* **2008**, *47*, 10813−10815. (g) Langley, S. K.; Chilton, N. F.; Gass, I. A.; Moubaraki, B.; Murray, K. S. *Dalton Trans.* **2011**, *40*, 12656−12659. (h) Lin, P.-H.; Burchell, T. J.; Ungur, L.; Chibotaru, L. F.; Wernsdorfer, W.; Murugesu, M. *Angew. Chem., Int. Ed.* **2009**, *48*, 9489−9492. (i) Andrews, P. C.; Deacon, G. B.; Gee, W. J.; Junk, P. C.; Urbatsch, A. *Eur. J. Inorg. Chem.* **2012**, 3273−3282. (j) Chandrasekhar, V.; Hossain, S.; Biswas, S.; Sutter, J.-P. *Inorg. Chem.* **2013**, *52*, 6346−6353.
(49) For recent literature on discrete Ln cubanes, see: (a) Gao, Y.; Xu, G.-F.; Zhao, L.; Tang, J.; Liu, Z. *Inorg. Chem.* **2009**, *48*, 11495−11497. (b) Ke, H.; Gamez, P.; Zhao, L.; Xu, G.-F.; Xue, S.; Tang, J. *Inorg. Chem.* **2010**, *49*, 7549−7557. (c) Liu, C.-M.; Zhang, D.-Q.; Hao, X.; Zhu, D.-B. *Cryst. Growth Des.* **2012**, *12*, 2948−2954. (d) Gerasko, O. A.; Mainicheva, E. A.; Naumova, M. I.; Yurjeva, O. P.; Antonio, A.; Vincent, C.; Llusar, R.; Fedin, V. P. *Eur. J. Inorg. Chem.* **2008**, 416−424. (e) Kong, X.-J.; Long, L.-S.; Zheng, L.-S.; Wang, R.; Zheng, Z. *Inorg. Chem.* **2009**, *48*, 3268−3273.
(50) (a) Guo, F.-S.; Leng, J.-D.; Lui, J.-L.; Meng, Z.-S.; Tong, M.-L. *Inorg. Chem.* **2012**, *51*, 405−413. (b) Bretonniere, Y.; Mazzanti, M.; Pecaut, J.; Bunand, F. A.; Merbach, A. E. *Inorg. Chem.* **2001**, *40*, 6737−6745. (c) Du, Z.; Zhang, Y.; Yao, Y.; Shen, Q. *Dalton Trans.* **2011**, *40*, 7639−7644. (d) Chandrasekhar, V.; Das, S.; Dey, A.; Hossain, S.; Sutter, J.-P. *Inorg. Chem.* **2013**, *52*, 11956−11965.
(51) (a) Koo, B. H.; Lim, K. S.; Ryu, D. W.; Lee, W. R.; Koh, E. K.; Hong, C. S. *Chem. Commun.* **2012**, *48*, 2519−2521. (b) Carretas, J.; Branco, J.; Marcalo, J.; Isolani, P.; Domingos, A.; de Matos, A. P. *J. Alloys Compd.* **2001**, *323*−*324*, 169−172. (c) Chen, Y.-H.; Tsai, Y.-F.; Lee, G.-H.; Yang, E.-C. *J. Solid State Chem.* **2012**, *185*, 166−171.
(52) MAGMUN4.1. and MAGMUN4.1/OW01.exe are available free of charge from the authors (http://www.ucs.mun.ca/∼lthomp/magmun.html).
(53) Lin, P.-H.; Sun, W.-B.; Tian, Y.-M.; Yan, P.-F.; Ungur, L.; Chibotaru, L.; Murugesu, M. *Dalton Trans.* **2012**, *41*, 12349−12352.
(54) (a) Pointillart, F.; Le Guennic, B.; Golhen, S.; Cador, O.; Maury, O.; Ouahab, L. *Chem. Commun.* **2013**, *49*, 615−617. (b) Abragam, A.; Bleaney, B. *Electron Paramagnetic Resonance of Transition Ions*; Dover Publications: New York, 1986.
(55) (a) Kahn, O. *Molecular Magnetism*; VCH Publishers: New York, 1993. (b) Benelli, C.; Gatteschi, D. *Chem. Rev.* **2002**, *102*, 2369−2388.
(56) (a) Chakov, N. E.; Wernsdorfer, W.; Abboud, K. A.; Christou, G. *Inorg. Chem.* **2004**, *43*, 5919−5930. (b) Mishra, A.; Tasiopoulos, A. J.; Wernsdorfer, W.; Abboud, K. A.; Christou, G. *Inorg. Chem.* **2007**, *46*, 3105−3115. (c) Papatriantafyllopoulou, C.; Stamatatos, Th. C.; Wernsdorfer, W.; Teat, S. J.; Tasiopoulos, A. J.; Escuer, A.; Christou, G. *Inorg. Chem.* **2010**, *49*, 10486−10496 and references cited therein..
(57) Brockman, J. T.; Stamatatos, Th. C.; Wernsdorfer, W.; Abboud, K. A.; Christou, G. *Inorg. Chem.* **2007**, *46*, 9160−9171.
(58) Katsoulakou, E.; Dermitzaki, D.; Konidaris, K. F.; Moushi, E. E.; Raptopoulou, C. P.; Psycharis, V.; Tasiopoulos, A. J.; Bekiari, V.; Manessi-Zoupa, E.; Perlepes, S. P.; Stamatatos, Th. C *Polyhedron* **2013**, *52*, 467−475.
(59) (a) Beedle, C. C.; Stephenson, C. J.; Heroux, K. J.; Wernsdorfer, W.; Hendrickson, D. N. *Inorg. Chem.* **2008**, *47*, 10798−10800. (b) Orfanoudaki, M.; Tamiolakis, I.; Siczek, M.; Lis, T.; Armatas, G. S.; Pergantis, S. A.; Milios, C. J. *Dalton Trans.* **2011**, *40*, 4793−4796. (c) Alexandropoulos, D. I.; Mowson, A. M.; Pilkington, M.; Bekiari, V.; Christou, G.; Stamatatos, Th. C. *Dalton Trans.* **2014**, *43*, 1965−1969.
(60) Dermitzaki, D.; Lorusso, G.; Raptopoulou, C. P.; Psycharis, V.; Escuer, A.; Evangelisti, M.; Perlepes, S. P.; Stamatatos, Th. C. *Inorg. Chem.* **2013**, *52*, 10235−10237.